The Compact Muon Solenoid Experiment

CMS Note
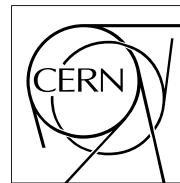
Summary of the CMS Discovery Potential for the MSSM SUSY Higgses

D. Denegri[a], V. Drollinger[b], R. Kinnunen[c], K. Lassila-Perini[c], S. Lehti[c], F. Moortgat[d], A. Nikitenko[e], S. Slabospitsky[f], N. Stepanov[g]

Abstract

This work summarises the present understanding of the expected MSSM SUSY Higgs reach for CMS. Many of the studies presented here result from detailed detector simulations incorporating final CMS detector design and response. With 30 fb^{-1} the $h \to \gamma\gamma$ and $h \to b\bar{b}$ channels allow to cover most of the MSSM parameter space. For the massive $A, H, H^{\pm}$ MSSM Higgs states the channels $A, H \to \tau\tau$ and $H^{\pm} \to \tau\nu$ turn out to be the most profitable ones in terms of mass reach and parameter space coverage. Consequently CMS has made a big effort to trigger efficiently on τ's. Provided neutralinos and sleptons are not too heavy, there is an interesting complementarity in the reaches for $A, H \to \tau\tau$ and $A, H \to \chi\chi$.

[a] European Laboratory for Particle Physics (CERN), Switzerland and DAPNIA, Saclay, France

[b] IEKP, Karlsruhe University, Germany - Now at Department of Physics and Astronomy, University of New Mexico, USA

[c] Helsinki Institute of Physics, Helsinki, Finland

[d] University of Antwerpen, Wilrijk, Belgium - Research Assistant of the FWO, Belgium

[e] Imperial College, University of London, London, UK - On leave from ITEP, Moscow, Russia

[f] IHEP, Protvino, Moscow Region, Russia

[g] European Laboratory for Particle Physics (CERN) - On leave from ITEP, Moscow, Russia

1   Introduction

For several years the LEP and the Tevatron have been functioning in an energy range allowing the direct search for the Higgs boson(s). LEP has recently been closed without solid evidence for the Higgs boson. The measurements yield as lower bounds 114.1 GeV for the Standard Model (SM) Higgs and 91.0 and 91.9 GeV for the light (h) and the pseudoscalar (A) Higgs bosons of the MSSM Model [1]. The excluded $tan\beta$ regions are $0.5 < tan\beta < 2.4$ for the maximal m_h scenario and $0.7 < tan\beta < 10.5$ for the no mixing scenario [1, 2]. The indirect searches, performing fits to all existing electroweak data indicate a light SM Higgs boson with the most probable mass m_H = 88 GeV+53 GeV-21 GeV and a 95% CL upper limit of 196 GeV [3]. Until the arrival of the LHC the only place where the Higgs search can be pursued in the coming yeares is at the Fermilab Tevatron. Integrated luminosities of from 20 to 40 fb^{-1} are needed to explore the $m_H \lesssim 170$ GeV range. This could possibly be achieved by 2007-2008 but evidence for the Higgs at the Tevatron in either the $H \to b\bar{b}$ or $H \to WW \to \ell\ell\nu\nu$ channels will be marginal. At LHC a clear signal for the Higgs boson can be expected already after few months of running ($\sim$ 10 fb^{-1}) in a part of the parameter space ($m_H \gtrsim 2m_Z$ for SM Higgs and high $tan\beta$ for MSSM Higgses). It is the region $m_H \lesssim 125$ GeV relying on $H \to \gamma\gamma$ and $H \to b\bar{b}$ channels which is the hardest, requiring $\gtrsim 30$ fb^{-1}. For the SM Higgs in the mass range from 125 to 180 GeV the channels $H \to ZZ^* \to 4\ell^{\pm}$ [4] and $H \to WW \to \ell\ell\nu\nu$ [5] are the most appropriate ones and require from 10 to 30 fb^{-1}.

In this note we present the summary of the expected reach for the following discovery channels of the MSSM Higgs bosons:

- $h \to \gamma\gamma$, inclusive production and production in association with an isolated lepton in Wh and $t\bar{t}h$ final states

- $h \to b\bar{b}$ in association with an isolated lepton and b-jets in Wh and $t\bar{t}h$

- $A, H \to \mu\mu$, inclusive and in $b\bar{b}H/A$ final states

- $A, H \to \tau\tau$ with $2\ lepton$, $lepton + \tau\ jet$ and $2\ \tau\ jet$ final states

- $H^{\pm} \to \tau\nu$ in $gb \to tH^{\pm}$ and in $q\bar{q}' \to H^{\pm}$

- $H^{\pm} \to tb$ in $gb \to tH^{\pm}$

- $A, H \to \chi_2^0\chi_2^0 \to 4\ell^{\pm} + X$

Several other channels have been investigated in CMS. Some of them, like $qq \to qqh$ with $h \to \tau\tau$, $h \to \gamma\gamma$ or $h \to WW$, are potentially very interesting and presently under study, but no conclusive results have been obtained yet. For other channels like $h, H \to ZZ^* \to 4\ell^{\pm}$, the discovery ranges are significantly less important or limited to the low $tan\beta$ region being thus either already excluded by the LEPII results or made less plausible.

The results presented in this note are not final ones but rather a snapshot of our present understunding, new developments are to be expected as the full simulation study with present and final CMS detector design and performance is going on or has to be started in the near future on most of the above channels.

2   Simulation tools

The PYTHIA versions 5.7 [6] and 6.1 [7] are used to generate physics events for the signals and for the backgrounds. With the PYTHIA version 5.7 the SUSY Higgs masses and couplings are corrected using calculations including two-loop/RGE improved radiative corrections [8]. Polarized τ decays are incorporated using the TAUOLA package [9]. In some cases the HDECAY package [10] is used to calculate or normalize the cross sections and branching ratios. Detector simulation is performed in general with the fast simulation package CMSJET [11]. However, the detector dependent issues like the resolutions of the narrow mass states, missing transverse energy resolution, b - and τ-tagging and jet resolution are studied with full GEANT-based (CMSIM and ORCA) detector simulation. The results are either used directly or parametrized for the fast simulation study.

3   MSSM Higgs bosons

With the assumption that the whole sparticle spectrum is heavy enough, the spectrum of the heavy MSSM Higgs bosons, the CP-odd (A), the CP-even (H) and the two charged ($H^{\pm}$) Higgs bosons, can be expressed with only two parameters, m_A and $tan\beta$. In the so-called decoupling limit, $m_A >> m_Z$, the heavy Higgs bosons become degenerate in mass. At tree-level the mass of the lightest CP-even Higgs boson h is bound to be lighter than the

Z, but the loop corrections to m_h are large and particularly sensitive to the mass of the top quark, SUSY scale and the amount of stop-quark mixing. With the recent calculations including two-loop radiative corrections the upper bound of m_h is ~ 113 GeV with no stop mixing and if the SUSY scale is taken to be 1 TeV, whilst for maximal stop mixing the upper bound is ~ 130 GeV. In the majority of our studies we assume the SUSY parameter spectrum used for the LEP benchmark scenarios [12]. For the no-mixing scenario the SUSY parameters are as follows: M_1 = 100 GeV, M_2 = 200 GeV, μ = -200 GeV, $M_{\tilde{g}}$ = 800 GeV, $M_{\tilde{q},\tilde{\ell}}$ = 1 TeV and A_t = 0. For the maximal m_h (maximal mixing) $A_t = \sqrt{6} \times M_{\tilde{q},\tilde{g},\tilde{\ell}}$ while the other parameters remain the same.

Figure 1 shows the total width of the CP-odd MSSM Higgs boson A as a function of m_A for $tan\beta$ values between 5 and 50 calculated with HDECAY [10]. Figure 2 shows the same for the CP-even MSSM Higgs boson H. The total width increases with increasing $tan\beta$ which in some cases may give the possibility to determine the value of $tan\beta$ from the width measurement. In CMS a sensitivity to two nearby states (A and H) few GeV apart, and possibly to the Higgs width measurement could be expected in the $A, H \to \mu\mu$ channel where effective mass resolution is at a percent level.

3.1 Branching ratios and cross sections

The branching ratios for $tan\beta = 5$ and $tan\beta = 40$ are shown in Figs. 3 and 4 for the heavy scalar H, in Figs. 5 and 6 for the pseudoscalar A and in Figs. 7 and 8 for the light scalar h calculated with the HDECAY [10] programs. Figures 9 and 10 show the same for the charged Higgs. The branching ratios for the heavy SUSY Higgs bosons are not sensitive to the amount of stop mixing and therefore the discovery ranges calculated with the branching ratios shown in these figures are valid also for the maximal mixing scenario. These branching ratios are insensitive also to the sign of the Higgsino mass parameter μ, which according to the recent indirect measurements [13], is more likely to be positive. In general the PYTHIA branching ratios agree with those shown in the figures. In some cases, like for $h \to \gamma\gamma$, there is a large disagreement between these two predictions and the HDECAY calculation is used.

The two most important production mechanisms for SUSY Higgs at the LHC are the inclusive gluon-gluon fusion $gg \to H_{SUSY}$ and the Higgs production in association with b-quarks $gg \to b\bar{b}H_{SUSY}$. As the Higgs coupling to b-quarks (and to τ's) is enhanced at high $tan\beta$ ($g_{Hb\bar{b}}, g_{H\tau\tau} \sim cos\beta^{-1}$) the associated production dominates at high $tan\beta$ values and is about 90% of the total rate for $tan\beta > 10$ and $m_H \gtrsim 300$ GeV. Thus the identification of b's and τ's is important for Higgs searches at LHC implying the need for good tracking and impact parameter measurements [14]. The gluon fusion is mediated by quark loops, which can be affected by mixing. Due to the dominance of the associated production and because only the CP-even Higgs can be affected, expectations for the heavy SUSY Higgs are not sensitive to the loop effects unlike the inclusive $h \to \gamma\gamma$ discussed in the following.

Figure 11 shows the cross sections for the CP-even SUSY Higgs bosons h and H as a function of the Higgs mass for $tan\beta = 30$ with the CTEQ4L structure functions calculated with the HIGLU [15] and HQQ [16] programs. The cross sections are shown separately for the $gg \to h/H$, $gg, qq \to b\bar{b}h/H$ and $qq \to qqh/H$ subprocesses. Figure 12 shows the corresponding predictions for the CP-odd Higgs A. The cross sections are compared with results from PYTHIA calculated with the same structure functios. The PYTHIA points for $gg, qq \to b\bar{b}H/A$ are systematically below the theoretical prediction indicating that in some cases our expectations may be conservative. The cross section for the charged Higgs in the process $bg \to tH^{\pm}$ is shown in Fig.13 as a function of $m_{H^{\pm}}$ for $tan\beta = 40$. The result of the calculation of ref. [42], shown also in the figure, includes both the $2 \to 2$ and $2 \to 3$ processes corrected for double counting. The PYTHIA prediction calculated using the process $bg \to tH^{\pm}$ alone overestimates the cross section at low $m_{H^{\pm}}$ by a factor of ~ 2.

4 Processes

4.1 $h \to \gamma\gamma$

The expected experimental sensitivity for the SM Higgs in the inclusive $H \to \gamma\gamma$ channel is evaluated with full simulation of the CMS electromagnetic calorimeter and $\gamma\gamma$ mass reconstruction, including conversion recovery [17, 18, 19]. Figure 14 shows the reconstructed Higgs mass superimposed on the total background for $m_H = 120$ GeV and for 100 fb^{-1}. The cross section times branching ratio required for a 5σ significance for 100 fb^{-1} is more than 40 fb for zero stop mixing ($m_h \lesssim 113$ GeV) and more than 30 fb for maximal stop mixing ($m_h \lesssim$

130 GeV). Higher cross sections are needed at lower mass values due to the increasing backgrounds. NLO cross sections are used for the signal and for the backgrounds.

The branching ratios for $h \to \gamma\gamma$ are calculated with the HDECAY program [10] and the $gg \to h$ cross section with the HIGLU package [15] including the next-to-leading order corrections (NLO). Figure 16 shows the expected discovery range as a function of m_A and $tan\beta$ for 100 fb^{-1} and for 30 fb^{-1} assuming no stop mixing. The cross section is calculated using only the gluon-gluon fusion process, which gives a conservative limit. Figure 17 shows the same in the maximal mixing scenario. The parameter space excluded by LEP [1] data is also shown in the figures.

It has been shown in refs. [20, 21] that the rate for $gg \to h \to \gamma\gamma$ could be strongly reduced in the case of large stop mixing if the stop becomes light, $m_{\tilde{t}_1} \lesssim 200$ GeV. The $\tilde{t}_1$ loop then interferes destructively with the top quark loop partially cancelling each other, which leads to a reduction of the $gg \to h$ cross section. The $h\gamma\gamma$ coupling is also affected, but since the dominant contribution comes now from a W loop, which interferes destructively with the top loop, a reduction of the top contribution by interfering stop loops increases the $h \to \gamma\gamma$ partial width. However, this positive loop contribution is smaller than the negative for $gg \to h$ and the net effect is a reduction of the overall $gg \to h \to \gamma\gamma$ rate.

The effect of light stop is studied using a modified HDECAY/HIGLU package [10]. Figure 18 shows the expected discovery range for $gg \to h \to \gamma\gamma$ assuming large mixing, $\tilde{A}_t = 1400$ GeV, and a light stop, $m_{\tilde{t}_1} = 300$ GeV as a function of m_A and $tan\beta$ for 30 fb^{-1} and for 100 fb^{-1} [22] compared with our standard expectation with heavy stop. The SUSY parameters μ and m_2 are taken to be $\mu = -250$ and $M_2 = 250$ GeV. For $m_{\tilde{t}_1} = 200$ GeV the reduction is so large that no discovery would be possible through the gluon fusion channel $gg \to h \to \gamma\gamma$. The only alternatives are then the tree-diagram associated production channels Wh and $t\bar{t}h$.

An excellent ECAL resolution is mandatory for the inclusive $h \to \gamma\gamma$ channel due to the large prompt $\gamma\gamma$ background ($S/B \sim 1/10$). The search of $h \to \gamma\gamma$ in the associated production channels Wh and $t\bar{t}h$ is less sensitive to the $\gamma\gamma$ mass resolution as in this case the backgrounds can be effectively reduced by the lepton requirement giving $S/B \sim 1/1$. However the event rate is small making these channels useful only at the ultimate luminosities, $Lt \gtrsim 100$ fb^{-1}. These channels are studied in ref. [23] with the fast detector simulation method. The expected discovery reach for $Lt \gtrsim 100$ fb^{-1} may exceed that for the inclusive channel at low $tan\beta$ values, as is shown in Figs. 16 and 17. The importance of the Wh and $t\bar{t}h$ channels is not only that they could be $H(h)$ discovery channels in case of suppressed $gg \to h$ production or difficulties in monitoring at a $\lesssim 1\%$ level the electromagnetic calorimeter calibration, but also because they provide measures of the WWH and $t\bar{t}H$ couplings.

4.2 $h \to b\bar{b}$

The $h \to b\bar{b}$ decay channel benefits from a large branching ratio over the whole m_A-$tan\beta$ parameter space, the same is true for the SM Higgs for $m_H \lesssim 130$ GeV. A detailed study of the $H \to b\bar{b}$ decay channel in WH and $t\bar{t}H$ events is presented in ref. [24] and in $t\bar{t}h$ events in refs. [25, 26]. To extract the Higgs signal in $t\bar{t}H \to l^{\pm}\nu q\bar{q}b\bar{b}b\bar{b}$ events requires tagging of up to 4 b-jets in the presence of a large hadronic activity, reconstruction of the Higgs mass from two b-jets and the reconstruction of the associated leptonic and hadronic top or the W. A sophisticated likelihood method has been developed in ref. [24] to optimise $H \to b\bar{b}$ signal visibility in the $t\bar{t}H$ channel. The main backgrounds ($t\bar{t}b\bar{b}$, $t\bar{t}jj$, $t\bar{t}Z$) are generated with the CompHep-PYTHIA package [27, 28] which includes the calculation of the matrix elements with higher order corrections. Figure 15 shows the reconstructed invariant mass for the SM Higgs boson superimposed on the total background for $m_H = 115$ GeV and for 30 fb^{-1}. The $t\bar{t}H$ channel is far more promising than the WH channel. The signal to background ratio in $t\bar{t}H$ is of the order of one and the discovery range is $m_H \lesssim 122$ GeV for 30 fb^{-1} (signal visibility degrades with increasing mass). Figures 16 and 17 show the expected discovery ranges for the MSSM Higgs in $t\bar{t}h$ final states in the no-mixing and in the maximal mixing (maximal m_h) scenario for 30 fb^{-1} and for 100 fb^{-1}. For observation of $H \to b\bar{b}$ in the WH channel, ultimate luminosities, in excess of $\gtrsim 200$ fb^{-1}, are needed due to the much lower signal to background ratio ($\sim 1/40$). The discovery reach for 300 fb^{-1} is at $m_H \lesssim 123$ GeV using lowest order calculations (k=1). The m_A-$tan\beta$ discovery contours for the Wh channel are similar to those for the $t\bar{t}h$, but about ten times more integrated luminosity is necessary to explore the same amount of parameter space. The importance of the $WH(Wh)$ channel is that it could provide a measure of the WWH coupling.

4.3 $A, H \to \mu\mu$

Although the branching ratio for $A, H \to \mu\mu$ is small, $\sim 3 \times 10^{-4}$, the associated $b\bar{b}H_{SUSY}$ production is enhanced at large $tan\beta$. This channel is very interesting as it allows a precise reconstruction of the Higgs boson mass thanks

3

to the excellent muon momentum resolution of CMS [29]. $A, H \rightarrow \mu\mu$ is studied in ref. [30] using for the muon momentum resolution results from a full simulation of the CMS tracker. The expected Higgs mass resolution for $m_A = 150$ GeV ($m_H = 151.2$ GeV) at $\tan\beta = 15$, for instance, is 2.2 GeV with superimposed unresolved CP-even (H) and CP-odd (A) states. B-tagging greatly improves signal visibility at large $\tan\beta$ reducing the overwhelming $Z, \gamma^* \rightarrow \mu\mu$ background. The expected discovery reach for 100 fb^{-1} is shown in Fig.21. At large $\tan\beta$ the natural width of A and H for accessible masses is in the few GeV to ~ 10 GeV range (Figs. 1, 2). With a $\sim 1\%$ level $\mu\mu$ mass resolution a fit to the $\mu\mu$ signal shape would allow measurement of its natural width.

4.4 $A, H \rightarrow \tau\tau$ with 2 $lepton$, $lepton + \tau$ jet and 2 τ jet final states

A systematic study of the $A, H \rightarrow \tau\tau$ decay with 2 $lepton$, $lepton + \tau$ jet and 2 τ jet final states is presently in progress in CMS including full simulation of the hadronic τ trigger, τ identification, τ tagging with impact parameter and vertex reconstruction, Higgs mass reconstruction and b-tagging in the associated production channels.

A detailed study of the $A, H \rightarrow \tau\tau$ with $e + \mu$ and $\ell^+\ell^-$ final states is presented in ref. [31]. Tagging of the associated b-jets and the impact parameter tagging of the two τ's are investigated with CMSIM simulation. The associated b-jets are soft and uniformly distributed in the central and endcap areas of the CMS tracker. The study shows that a b-tagging efficiency of $\sim 35\%$ can be obtained for these b-jets keeping the mistagging rate in the $Z + jets$ events under 1% level. Promising results are also obtained for τ tagging through impact parameter measurements of the two hard leptons from the τ decays. Tau tagging is needed to suppress the backgrounds where the leptons originate from W or Z. This method allows to double the signal statistics by including all $\ell^+\ell^-$ and not only $e + \mu$ final states. The expected discovery range is shown in Figs. 19 and 20 for 30 fb^{-1} and in Fig. 21 for 100 fb^{-1} separately for the $e + \mu$ and $\ell^+\ell^-$ final states. Examples of the $e + \mu$ - and $\ell^+\ell^-$ signals are shown in Figs. 22 and 23.

$A, H \rightarrow \tau\tau$ with 2 τ jet hadronic final sates have been shown to extend significantly the SUSY Higgs discovery reach into the large mass (600 - 800 GeV) range [32]. To exploit fully the 2 τ jet final states - especially in the low (~ 200 GeV) mass range - an efficient hadronic τ trigger has been developped based on Level-1 calorimeter selection, Level-2 electromagnetic calorimeter isolation and collimation [33] and a Level-3 tracking (isolation) in the pixel detector [34]. A reduction factor of $\sim 10^3$ against the QCD background is obtained with the full High Level Trigger selection (Level2 and Level3) with an efficiency of $\sim 35\%$ for the signal at $m_H = 200$ and 500 GeV [35].

Offline τ identification in the hadronic final states is based on a requirement of an isolated hard ($p_t > 40$ GeV) charged track inside the jet. This τ selection gives a rejection factor of $\sim 3 \times 10^{-4}$ against a QCD jet with $E_t \sim$ 100 - 200 GeV. A significant improvement can be expected from the impact parameter measurement of the two hard tracks as discussed above in the case of the $\ell^+\ell^-$ final states. Furthermore, including the τ to 3-prong decays in a small cone in the core of the calorimetric jet, the event rate for $A, H \rightarrow \tau\tau \rightarrow 2$ τ jets is enhanced by a factor of ~ 1.7. The rejection factor against the QCD jets degrades by a factor of ~ 3 when the 3-prong decays are included. However this background may also be suppressed by secondary vertex reconstruction. Promising results are obtained from a study on the identification of the 3-prong τ vertex with full (ORCA) track reconstruction [36]. A rejection factor of ~ 5 is obtained against the 3-prong QCD jets with an efficiency of $\sim 70\%$ for the τ jets.

The resolution of the reconstructed Higgs mass and even more so the mass reconstruction efficiency in $A, H \rightarrow \tau\tau$ events is very sensitive to the E_t^{miss} measurement. The absolute value of E_t^{miss} is relatively small in these events making the mass reconstruction and background reduction with a cut in E_t^{miss} a difficult task. Most recent results from full simulation [37] indicate a good mass resolution and reconstruction efficiency and confirm the earlier results of the fast simulation study [32]. The expected discovery reaches for the 2 τ jet and the $lepton + \tau$ jet [38] final states are shown in Figs. 19 (no mixing) and 20 (maximal mixing) for 30 fb^{-1}.

4.5 $H^\pm \rightarrow \tau\nu$ in $gb \rightarrow tH^\pm$ and in $q\overline{q'} \rightarrow H^\pm$

Search for the charged Higgs at LHC is essential for the understanding of the nature of the Higgs sector. $H^\pm \rightarrow \tau\nu$ with a hadronic τ decay has been shown to lead to the most favourable signature. The signal can be strongly enhanced against the background from $W \rightarrow \tau\nu$ decays exploiting the τ polarization in the one-prong $\tau \rightarrow \pi^\pm(\pi^0)\nu$ decays [39]. Due to the τ polarization, the single pion from a τ decay is harder when the τ originates from an $H^\pm$ than from a W. Requiring 80% of the visible τ-jet energy to be carried by the single pion, the $t\overline{t}$ background can be reduced by a factor of ~ 300 while keeping the signal efficiencies at a 10% to 20% level (including the jet E_t threshold) [40].

If the charged Higgs is light, $m_{H+} < m_{top}$, the production is through the the the $t\bar{t}$ events followed by $t \to H^{\pm}b$ and the discovery range is limited by the top mass [41]. The expected discovery range for 30 fb^{-1} is for $m_A \lesssim$ 160 GeV almost independent of $tan\beta$ and is shown in Fig. 19. For a heavier charged Higgs, $m_{H+} > m_{top}$, the main production processes are $gg \to tbH^{\pm}$, $gb \to tH^{\pm}$ and $q\bar{q} \to H^{\pm}$; the two first processes partially overlap with a b from the proton structure. The production in association with the top quark is shown to lead to the most favourable final states if purely hadronic final states $t \to qqb$ are selected, with an almost background-free signal in the transverse mass reconstructed from the τ jet and the transverse missing energy [39, 40]. Figure 24 shows the reconstructed transverse mass for $m_{H^{\pm}} = 217$ GeV ($m_A = 200$ GeV) and $tan\beta = 40$ superimposed on the total background for $30 fb^{-1}$. Determination of the Higgs mass from the endpoint may be possible with a $\sim 2\%$ precision. Results of ref. [40] are obtained using the PYTHIA6.1 cross sections and branching ratios which are found to be in a rough agreement with the theoretical expectations [42]. The expected discovery reach is shown in Figs. 19 for 30 fb^{-1} and in Fig. 21 for 100 fb^{-1}.

The s-channel production of $H^{\pm}$ in $q\bar{q}' \to H^{\pm} \to \tau\nu$ is investigated using again the hadronic τ decay and exploiting the τ polarization method discussed above [43]. It is difficult to obtain a signal as the reconstructed $H^{\pm}$ transverse mass is on the tail of the very large $q\bar{q}' \to W \to \tau\nu$ background. It is shown in ref. [43] that nevertheless the Higgs mass and $tan\beta$ may be still extracted using fits to the transverse mass distributions. The expected discovery reach is shown in Figs. 19 and 20 for 30 fb^{-1}.

4.6 $H^{\pm} \to tb$ in $gb \to tH^{\pm}$

The other important decay channel of the charged Higgs, $H^{\pm} \to tb$, has been investigated recently in $gb \to tH^{\pm}$ production, requiring one isolated lepton from the decay of one of the top quarks [45]. To extract the Higgs signature in these multijet events requires tagging of three b-jets, reconstruction of the leptonic and hadronic top quark and the Higgs mass reconstruction from a top quark and one b-jet. The study is made with a realistic b-tagging simulation based on the CMSIM reconstruction of the CMS tracker, and taking into account the correct kinematics of the jets in the event. After selection cuts and b-tagging, the background is concentrated in the signal area making the identification of the Higgs mass peak difficult in this channel. The expected discovery range at high $tan\beta$ is shown in Fig. 19 for 30 fb^{-1}.

4.7 $A, H \to \chi_2^0\chi_2^0 \to 4\ell^{\pm} + X$

As can be seen from Figs. 19 - 21, essentially the whole MSSM m_A-$tan\beta$ parameter space not excluded by LEP is expected to be covered by the light SUSY Higgs signal with $h \to \gamma\gamma$ and $h \to b\bar{b}$ decays in both the no-mixing and maximal m_h scenarios already with 30 fb^{-1}. At high $tan\beta$ the heavy SUSY Higgses are expected to be found with the decays to τ's and muons, the discovery ranges extending down to $tan\beta \sim 10$ for the low mass range $m_A \lesssim$ 200 GeV and to $tan\beta \sim 20$ for the high mass range $m_A \gtrsim 300$ GeV. If $tan\beta$ is between these boundaries and the LEPII limit it may be difficult to identify the nature (SM or SUSY) of the only $h \to \gamma\gamma$ or $h \to b\bar{b}$ discovered Higgs state. It is shown in ref. [44] that in this part of the m_A-$tan\beta$ parameter space Higgs decays to sparticles (Figs. 3-5) can be used to complete the search with SM particle decays. The channel $A, H \to \chi_2^0\chi_2^0 \to 4\ell^{\pm} + X$ turns out to be the most favourable one provided neutralinos and sleptons are light enough so that the $\chi_2^0(\to \tilde{\ell}\ell) \to \chi_1^0\ell^+\ell^-$ branching ratio is significant. The four isolated lepton final state signature with little additional jet activity allows to reduce drastically the background levels. For this channel the backgrounds coming from other SUSY processes dominate and have to be taken into account. Figure 25 shows the signal in the 4-$lepton$ channel with all expected SM and SUSY backgrounds at a favourable point in parameter space $m_A = 350$ GeV and $tan\beta = 5$ and with the following MSSM parameters: $M_1 = 60$ GeV, $M_2 = 120$ GeV, $\mu = $ -500 GeV, $M_{\tilde{q},\tilde{g}} = 1000$ GeV, $M_{\tilde{\ell}} = 250$ GeV and $A_t = 0$. The expected m_A-$tan\beta$ reach for 30 fb^{-1} and 100 fb^{-1} is shown in Fig. 26. This parameter choice does not affect the discovery ranges for the Higgs decays to SM particles at intermediate and high $tan\beta$ values as the branching ratios do not change significantly provided $m_{\tilde{q}}$ and $m_{\tilde{g}}$ remain heavy [46]. The expected m_A-$tan\beta$ reach for the $\chi_2^0\chi_2^0$ channel is shown in Fig. 26 for 30 fb^{-1} and 100 fb^{-1}. The figure also illustrates that if the neutralinos are heavier ($M_2 = 180$ GeV) the reach is reduced because of the mass threshold effect.
Figure 27 shows the expected m_A-$tan\beta$ reach for the heavy SUSY Higgs bosons including this channel and the channels with SM particle decays for 100 fb^{-1} assuming $M_1 = 90$ GeV, $M_2 = 180$ GeV, $\mu = 500$ GeV, $M_{\tilde{q},\tilde{g}} = 1000$ GeV and $M_{\tilde{\ell}} = 250$ GeV. The complementarity of searches of A and H decays to SM and SUSY particles is clear comparing Figs. 21 and 27.

5 Conclusions

The expected discovery ranges for the MSSM Higgs bosons are summarized in Figs. 19 - 27. Only the main discovery channels investigated in detail in CMS are shown and discussed in this note. The whole parameter space not excluded by LEP is expected to be covered with the light Higgs decay modes $h \to \gamma\gamma$ and $h \to b\bar{b}$ in the no-mixing case already with 30 fb^{-1}. If the stop mixing is maximal a tiny corner of the parameter space between the discovery ranges for the light charged Higgs in $t\bar{t}$ events and for the $h \to b\bar{b}$ channel around $m_A \sim 120$ GeV and $tan\beta \sim 5$ is still left unexplored with 30 fb^{-1}. With 60 fb^{-1} the $h \to b\bar{b}$ channel extends towards lower m_A values and closes this area. The heavy neutral MSSM Higges are expected to be discovered at high $tan\beta$ in the $H, A \to \mu\mu$ and $H, A \to \tau\tau$ decays. The final states of 2 $leptons$, $lepton + \tau$ jet and 2 τ $jets$ are investigated for $H, A \to \tau\tau$ decays. The 2 τ jet final states are found to extend the reach significantly towards the high Higgs masses and to provide the best $\tau\tau$ mass resolution ($\sim 14\%$). The $A, H \to \chi_2^0\chi_2^0 \to 4\ell^{\pm} + X$ channel can complement the $\tau\tau$ channel at low $tan\beta$ provided neutralinos and sleptons are light enough. For the search of the charged Higgs, the $H^{\pm} \to \tau\nu$ decay in $gb \to tH^{\pm}$ events with fully hadronic final states is found to be the most favourable.

Investigations on several other channels, not discussed above, are in progress in CMS. Among the most interesting ones are the studies on the weak boson fusion channels $qq \to qqH$ which are essential for the measurement of the WWH and $\tau\tau H$ couplings and the total width of the Higgs boson [47]. These channels with $h \to \tau\tau$ and $H \to \tau\tau$ decays could possibly cover the whole MSSM parameter space [48]. Promising results are also obtained for the $H \to \gamma\gamma$ channel with a fast simulation method [49]. As the event rates in all these qqH channels are small, and as the Higgs mass reconstruction and the forward jet tagging are highly detector sensitive, a full simulation is really needed before definite conclusions can be made. Such studies are now under way for the $H(h) \to \tau\tau$ [50], $H(h) \to WW \to \ell\ell\nu\nu$ [51] and $h \to \chi^0\chi^0$ (invisible Higgs) [52] channels.

6 Acknowledgements

References

[1] The ALEPH, DELPHI, L3 and OPAL Collaborations, and the LEP Higgs Working Group, CERN-EP/2001-055 and hep-ex/0107030.

[2] T. Junk and V. Ruhlmann-Kleider, Private communication.

[3] The LEP Electroweak Working Group, A Combination of Preliminary Electroweak Measuremets and Constraints in the Standard Model, CERN-EP/2001- in preparation, presented by D. Charlton, EPS HEP 2001, Budapest, Hungary, July 12-18, 2001.

[4] Ivica Puljak, Potentiel de decouverte du boson de Higgs dans le canal $H \rightarrow ZZ^* \rightarrow 4\ell^{\pm}$ avec le detecteur CMS. Contribution a la construction du calorimetre electromagnetique de CMS, These de Doctorat de l'Universite Paris VI, Septembre 2000.

[5] M. Dittmar, hep-ex/9901009.

[6] T. Sjostrand, Comp.Phys.Comm. 82 (1994) 74; CERN-TH.6488/92; CERN-TH.7112/93.

[7] T. Sjostrand, P. Eden, Ch. Friberg, L. Lonnblad, C. Miu, S. Mrenna and E. Norrbin, High-Energy-Physics Event Generation with PYTHIA 6.1, Computer Phys. Commun. 135 (2001) 238.

[8] J.F. Gunion, A. Stange and S. Willenbrock, Weakly-coupled Higgs Bosons, UCD-95-28,hep-ph/9602238

[9] S. Jadach, Z. Was, R. Decker, M. Jezabek and J.H. Kuhn, CERN-TH-6793, 1992.

[10] A. Djouadi, J. Kalinowski and M. Spira, HDECAY: a program for Higgs Boson Decays in the Standard Model and its Supersymmetric expension, hep-ph/9704448.

[11] S. Abdullin, A. Khanov and N. Stepanov, CMSJET, CMS TN/94-180.

[12] M. Carena, S. Heynemeyer, C.E.M. Wagner and G. Weiglein, Suggestions for improved benchmark scenarios for Higgs-boson searches at LEP2, CERN-TH/99-374, DESY 99-186, hep-ph/9909435.

[13] Muon (g-2) Collaboration, H. N. Brown et al., Phys. Rev. Lett. 86 (2001) 2227.

[14] CMS Collaboration, The tracker project, Technical Design Report, CERN/LHCC 98-6, CMS TDR 5, 26 February 1998.

[15] M. Spira, Higlu : a program for the calculation of the total Higgs production cross section at hadron colliders via gluon fusion including QCD corrections, hep-ph/9510347.

[16] M. Spira, PPHTT, program to calculate cross sections for processes $gg \rightarrow b\bar{b}H_{SUSY}, t\bar{t}H_{SUSY}$, http://m.home.cern.ch/m/mspira/www/hqq/.

[17] CMS Collaboration, The electromagnetic calorimeter project, Technical Design Report, CERN/LHCC 97-33, CMS TDR 4, 15 December 1997.

[18] C. Seez, privite communication.

[19] Katri Lassila-Perini, Discovery Potential of the Standard Model Higgs in CMS at the LHC, Diss. ETH N.12961.

[20] A.Djouadi, Phys. Lett. B435 (1998) 101

[21] A. Djouadi, Squark effects on Higgs boson production and decay at the LHC, hep-ph/9806315

[22] R. Kinnunen, S. Lehti, A. Nikitenko and S. Rantala, Effects of large mixing and light stop for $h \rightarrow \gamma\gamma$ in MSSM, CMS NOTE 2000/043.

[23] M. Dzelalija, Z. Antunovic, D. Denegri and R. Kinnunen, Study of the Associated production Modes $Wh, t\bar{t}$ in the Minimal Supersymmetric Standard Model in CMS, CMS TN/96-091.

[24] Volker Drollinger, Reconstruction and Analysis Medhods for Searches of Higgs Bosons in the Decay Mode $H \rightarrow b\bar{b}$ at Hadron Colliders, Dissertation, Institut fur Experimentelle Kernphysik, University of Karlsruhe, Germany, July 2001.

[25] V. Drollinger, Th. Muller and D. Denegri, Searching for Higgs Bosons in Association with Top Quark Pairs in the $H \rightarrow b\bar{b}$ Decay Mode, CMS NOTE 2001/054, hep-ph/0111312.

[26] D. Green, K. Maeshima, R. Vidal, W. Wu and S. Kunori, A Study of ttbar + Higgs at CMS, CMS NOTE-2001/039.

[27] A. Pukhov, E. Boos, M. Dubinin, V. Edneral, V. Ilyin, D. Kovalenko, A. Kryukov, V. Savrin, S. Shichanin and A. Semenov, CompHEP - a package for evaluation of Feynman diagrams and integration over multi-particle phase space, INP-MSU 98-41/542.

[28] A. S. Belyaev, E. E. Boos, A. N. Vologdin, M. N. Dubinin, V. A. Ilyin, A. P. Kryukov, A. E. Pukhov, A. N. Skachkova, V. I. Savrin, A. V. Sherstnev, S. A. Shichanin, CompHEP-PYTHIA interface: integrated package for the collision events generation based on exact matrix elements, hep-ph/0101232

[29] CMS Collaboration, The muon project, Technical Design Report, CERN/LHCC 97-32, CMS TDR 3, 15 December, 1997.

[30] I.K. Furic and R. Kinnunen, Study of $H, A \rightarrow \mu\mu$ in CMS, CMS NOTE 1998/039.

[31] Sami Lehti, Prospects for the Detection of the MSSM Higgs Bosons Decaying into Tau Leptons in the CMS Detector, Dissertation, University of Helsinki, Report Series in Physics, HU-P-D93, 2001.

[32] R. Kinnunen and D. Denegri, Study of $H, A \rightarrow \tau\tau \rightarrow h^+ + h - +X$ in CMS, CMS NOTE 1999/037.

[33] S. Eno, W. Smith, S. Dasu, R. Kinnunen and A. Nikitenko, A Study of a First and Second Level Tau Trigger, CMS NOTE 2000/055.

[34] D. Kotlinski, A. Nikitenko and R. Kinnunen, Study of a Level-3 Tau Trigger with the Pixel Detector, CMS NOTE 2001/017.

[35] A. Nikitenko, CMS NOTE in preparation.

[36] A. Nikitenko and L. Wendland, Talk in the btau Meeting, 21 August, 2001.

[37] A. Nikitenko, S. Kunori and R. Kinnunen, Missing Transverse Energy Measurement with Jet Energy Corrections, CMS NOTE 2001/040.

[38] R. Kinnunen and A. Nikitenko, Study of $H, A \rightarrow \tau\tau \rightarrow \ell + \tau jet + E_t^{miss}$ in CMS, CMS NOTE 1997/106.

[39] D.P. Roy, The Hadronic Tau Decay Signature of Heavy Charged Higgs Boson at LHC, Phys. Lett. B459(1999)607.

[40] R. Kinnunen, Study of Heavy Charged Higgs in $pp \rightarrow tH^{\pm}$ with $H^{\pm} \rightarrow \tau\nu$ in CMS, CMS NOTE 2000/045.

[41] S. Banerjee, M. Mainty, Search for Charged Higgs in Top Decays in CMS, CMS NOTE 2000/039.

[42] S. Moretti and D.P. Roy, Detecting Heavy Charged Higgs Boson at LHC with Triple B-tagging, hep-ph/9909435.

[43] S. Slabospitsky, CMS NOTE in preparation.

[44] S. Abdullin, D. Denegri and F. Moortgat, Observability of MSSM Higgs bosons via sparticle decay modes in CMS, CMS NOTE 2001/042;
F. Moortgat, Observability of MSSM Higgs bosons decaying to sparticles at the LHC, CMS CR 2001/005.

[45] P. Salmi, R. Kinnunen and N. Stepanov, CMS NOTE in preparation.

[46] M. Spira, private communication.

[47] D. Zeppenfeld, R. Kinnunen, A. Nikitenko and E. Ricter-Was, Phys. Rev. D 62 (2000) 013009.

[48] D. Rainwater and D. Zeppenfeld, Journal of High Energy Phys. 12 (1997) 005.

[49] M. Dubinin, Higgs Boson Signal in the Reaction $pp \rightarrow Gamma\ Gamma + 2\ Forward\ Jets$, CMS NOTE 2001/022.

[50] A. Nikitenko, Tau Trigger for Higgs Studies at CMS, Invited Talk given in Higgs and Supersymmetry, Orsay, March 19-22, 2001.

[51] A. Nikitenko et al., CMS NOTE in preparation.

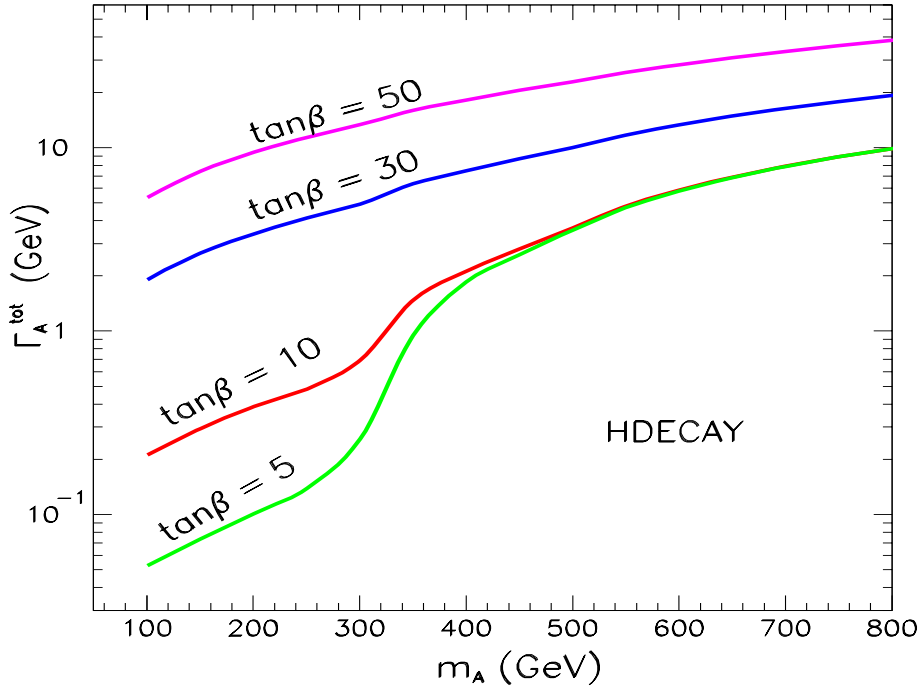[52] K. Mazumdar and A. Nikitenko, CMS NOTE in preparation.

Figure 1: Total width of the A^0 boson as a function of m_A for $tan\beta = 5$ to $tan\beta = 50$ calculated with HDECAY [10].
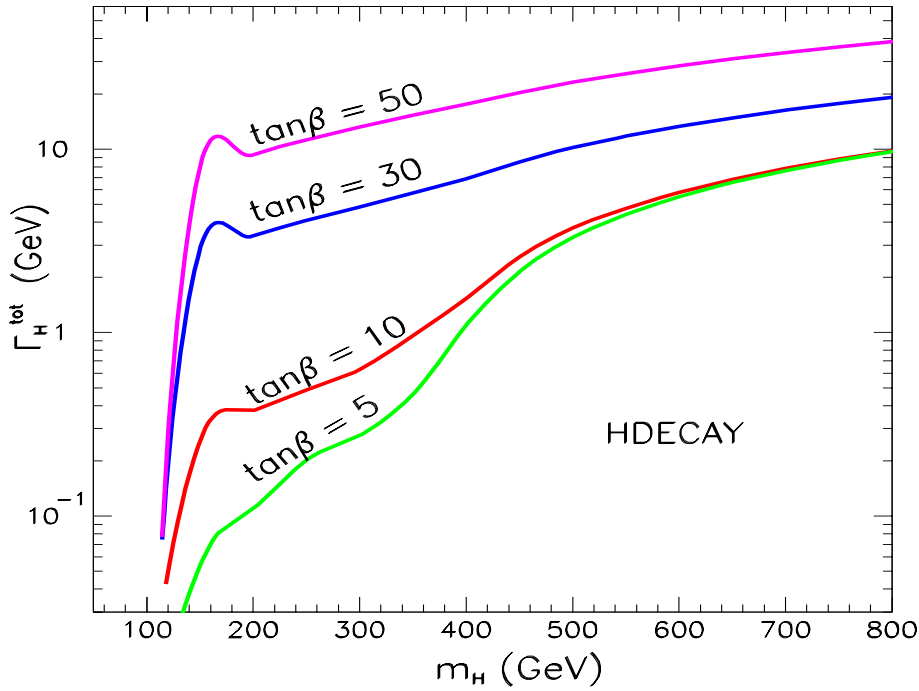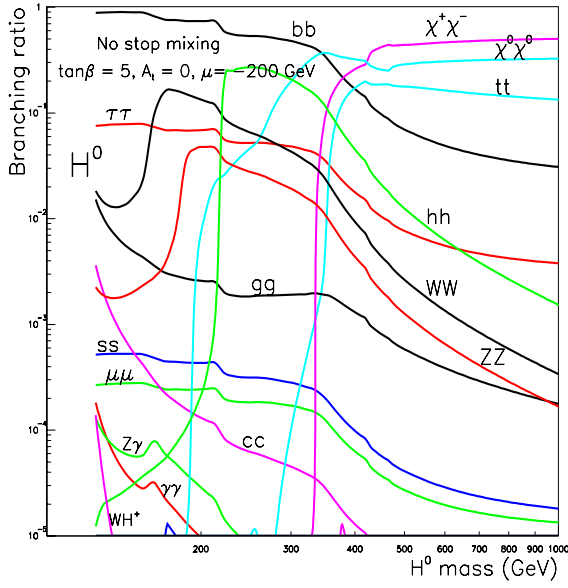

Figure 2: Total width of the H^0 boson as a function of m_H for $tan\beta = 5$ to $tan\beta = 50$ calculated with HDECAY [10].

Figure 3: Branching ratio for H^0 as a function of m_H for $tan\beta = 5$ calculated with HDECAY [10]. The SUSY parameters are taken to be $A_t = 0$ (no-mixing), $M_2 = 200$ GeV, $\mu = $ -200 GeV and $M_{\tilde{q},\tilde{\ell},\tilde{g}} = 1$ TeV.
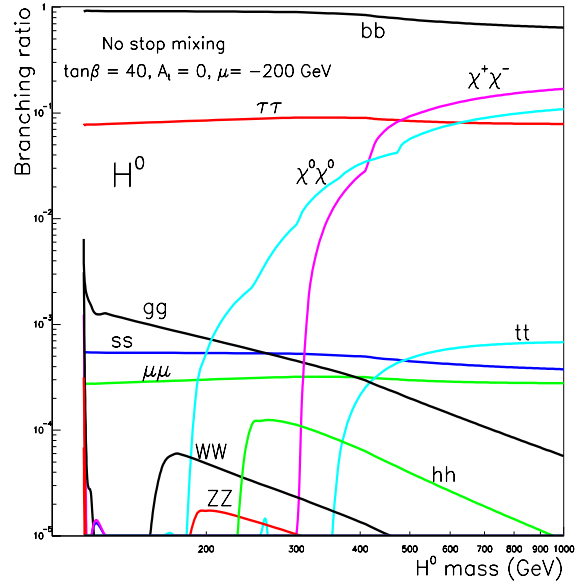
Figure 4: Branching ratio for H^0 as a function of m_H for $tan\beta = 40$ calculated with HDECAY [10]. The SUSY parameters are taken to be $A_t = 0$ (no-mixing), $M_2 = 200$ GeV, $\mu = $ -200 GeV and $M_{\tilde{q},\tilde{\ell},\tilde{g}} = 1$ TeV.
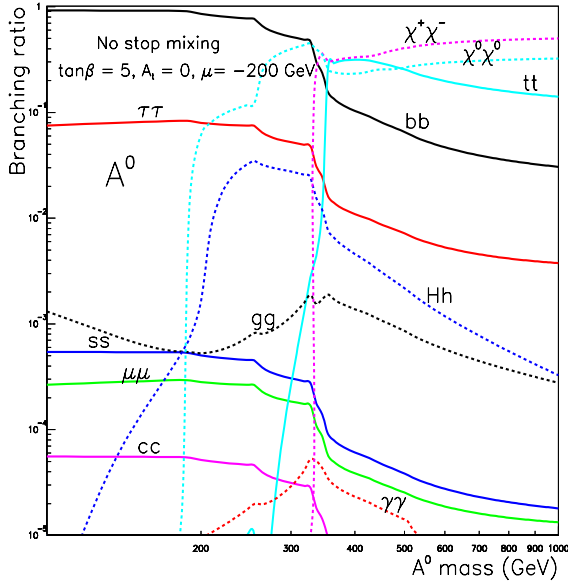
Figure 5: Branching ratio for A^0 as a function of m_A for $tan\beta = 5$ calculated with HDECAY [10]. The SUSY parameters are taken to be $A_t = 0$ (no-mixing), $M_2 = 200$ GeV, $\mu = $ -200 GeV and $M_{\tilde{q},\tilde{\ell},\tilde{g}} = 1$ TeV.
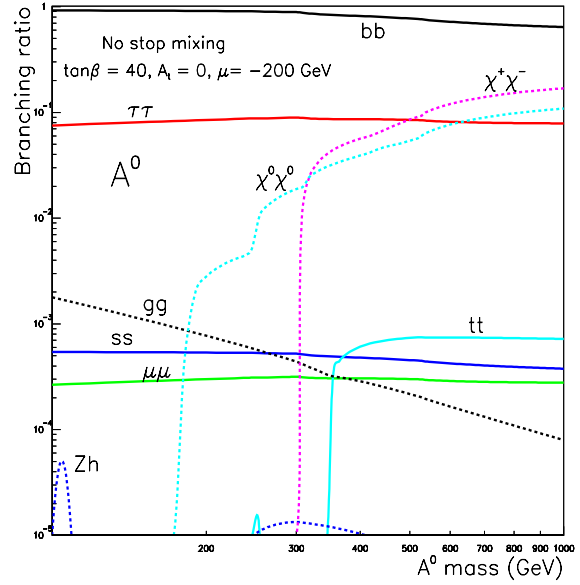
Figure 6: Branching ratio for A^0 as a function of m_A for $tan\beta = 40$ calculated with HDECAY [10]. The SUSY parameters are taken to be $A_t = 0$ (no-mixing), $M_2 = 200$ GeV, $\mu = $ -200 GeV and $M_{\tilde{q},\tilde{\ell},\tilde{g}} = 1$ TeV.

11
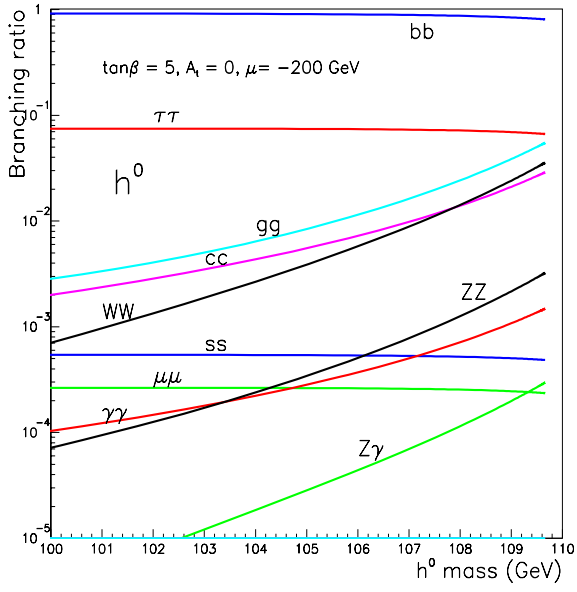
Figure 7: Branching ratio for h^0 as a function of m_h for $tan\beta = 5$ calculated with HDECAY [10]. The SUSY parameters are taken to be $A_t = 0$ (no-mixing), $M_2 = 200$ GeV, $\mu = $ -200 GeV and $M_{\tilde{q},\tilde{\ell},\tilde{g}} = 1$ TeV.
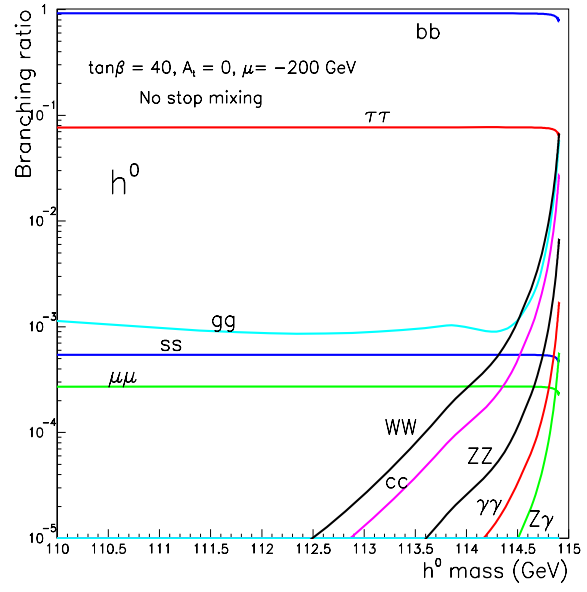
Figure 8: Branching ratio for h^0 as a function of m_h for $tan\beta = 40$ calculated with HDECAY [10]. The SUSY parameters are taken to be $A_t = 0$ (no-mixing), $M_2 = 200$ GeV, $\mu = $ -200 GeV and $M_{\tilde{q},\tilde{\ell},\tilde{g}} = 1$ TeV.
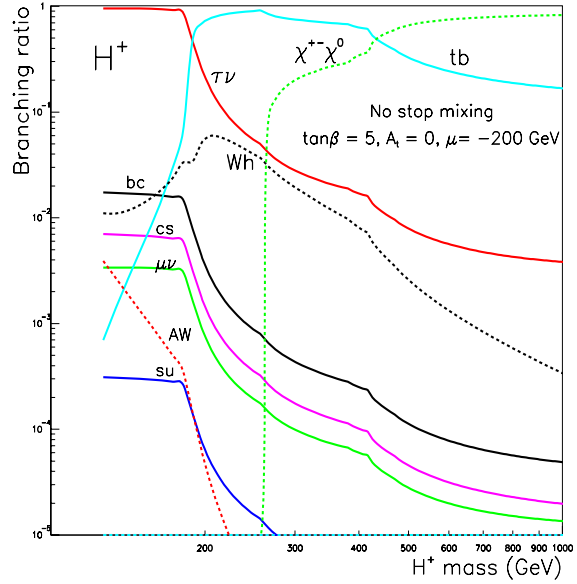
Figure 9: Branching ratio for $H^{\pm}$ as a function of $m_{H^{\pm}}$ for $tan\beta = 5$ calculated with HDECAY [10]. The SUSY parameters are taken to be $A_t = 0$ (no-mixing), $M_2 = 200$ GeV, $\mu = $ -200 GeV and $M_{\tilde{q},\tilde{\ell},\tilde{g}} = 1$ TeV.
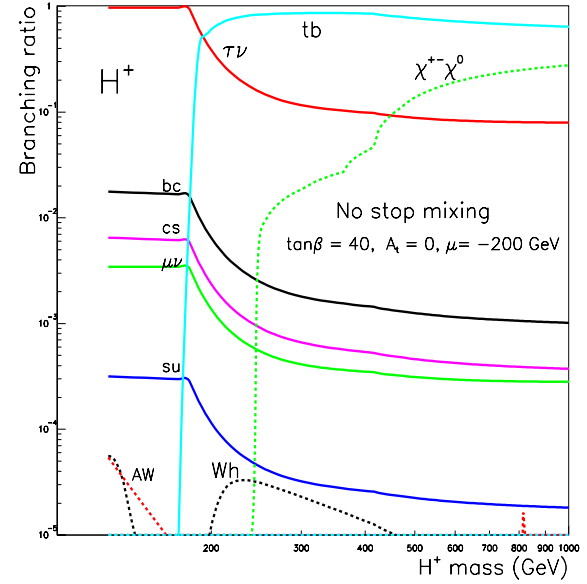
Figure 10: Branching ratio for $H^{\pm}$ as a function of $m_{H^{\pm}}$ for $tan\beta = 40$ calculated with HDECAY [10]. The SUSY parameters are taken to be $A_t = 0$ (no-mixing), $M_2 = 200$ GeV, $\mu = $ -200 GeV and $M_{\tilde{q},\tilde{\ell},\tilde{g}} = 1$ TeV.

12
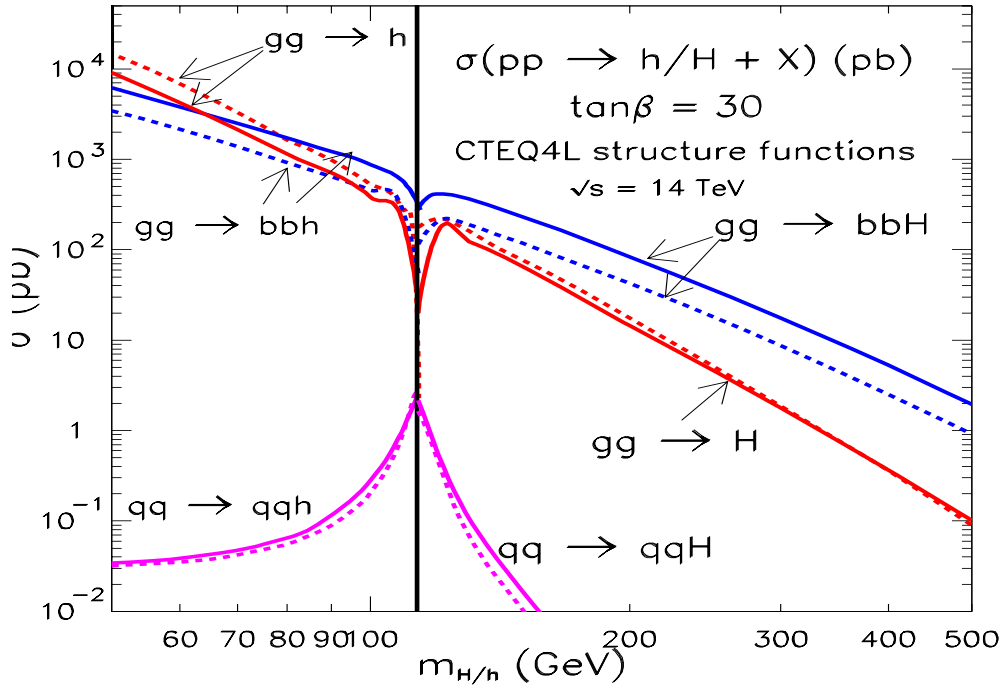
Figure 11: Cross sections for $gg \rightarrow H, h$, $gg \rightarrow b\bar{b}H, h$ and $qq \rightarrow qqH, h$ as a function of the Higgs mass for $tan\beta = 30$ with the CTEQ4L structure functions calculated with HIGLU/HQQ package [15]. The dashed lines are from PYTHIA6.1 with the same structure functions.
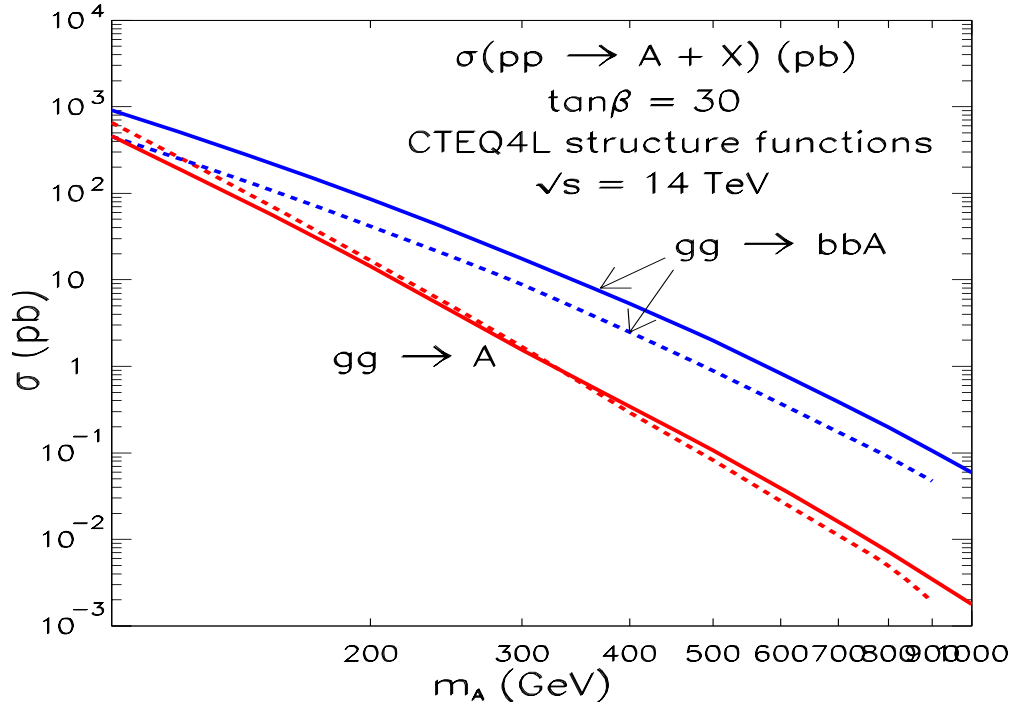
Figure 12: Cross sections for $gg \rightarrow A$ and $gg \rightarrow b\bar{b}A$ as a function of the Higgs mass for $tan\beta = 30$ with the CTEQ4L structure functions calculated with HIGLU/HQQ package [15]. The dashed lines are from PYTHIA6.1 with the same structure functions.
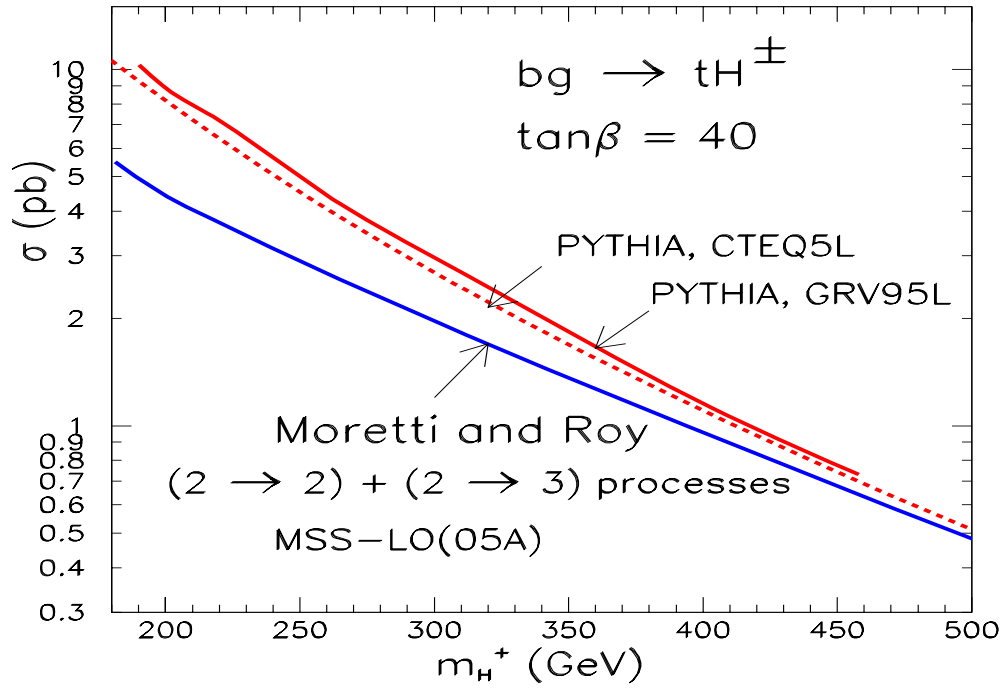
Figure 13: Cross section for $gb \rightarrow tH^{\pm}$ for $tan\beta = 40$ compared with the theoretical prediction of ref. [42].
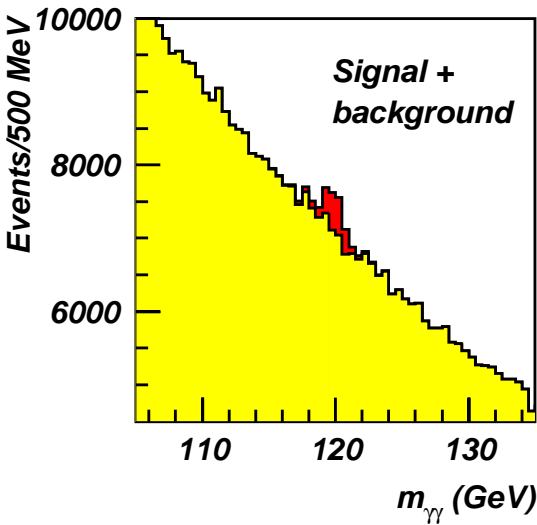
Figure 14: Reconstructed Higgs mass for $H \rightarrow \gamma\gamma$ superimposed on the total background for $m_H = 120$ GeV with 100 fb^{-1}.
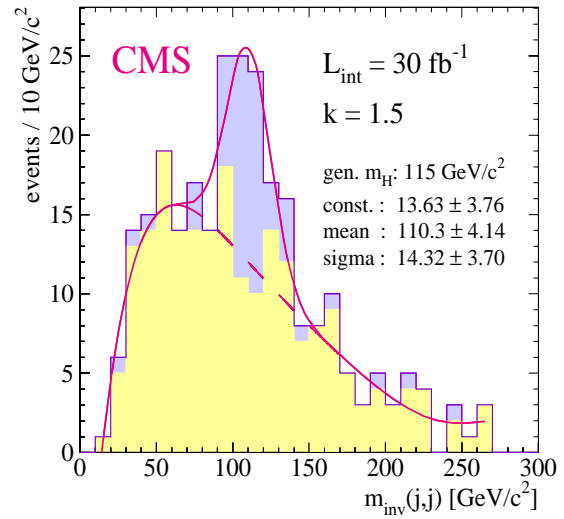
Figure 15: Reconstructed Higgs mass for $t\bar{t}H$, $H \rightarrow b\bar{b}$ superimposed on the total background for $m_H = 115$ GeV with 30 fb^{-1}.
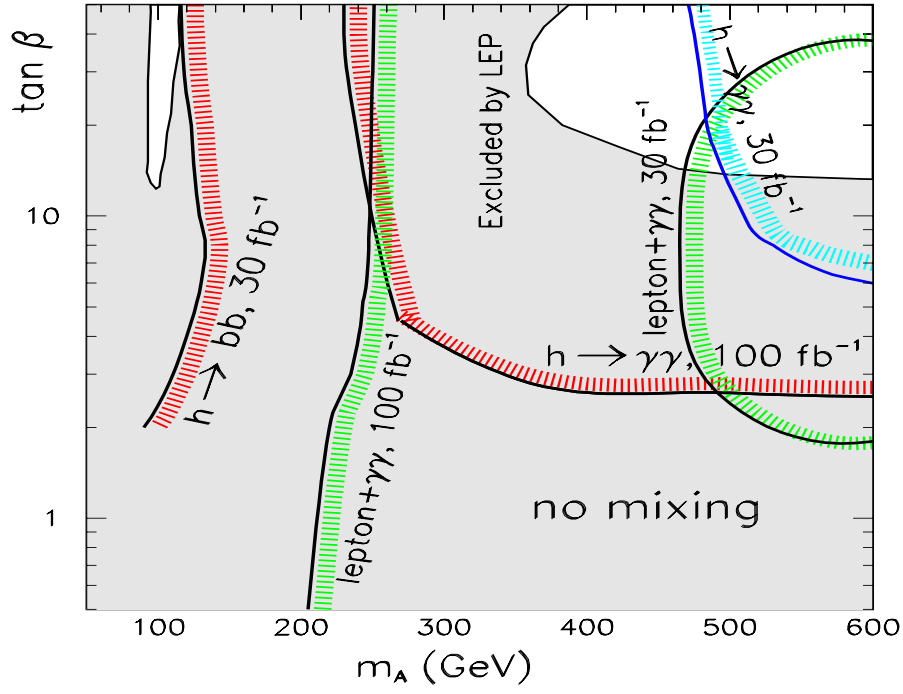
Figure 16: Expected 5σ discovery reach for the inclusive $gg \to h \to \gamma\gamma$ for 30 and 100 fb^{-1} and for $\ell\gamma\gamma$ in $t\bar{t}h$ and Wh production and for $h \to b\bar{b}$ in $t\bar{t}h$ production for 30 fb^{-1} as a function of m_A and $tan\beta$ in the no-mixing scenario. The shaded area is excluded by LEP [1, 2].
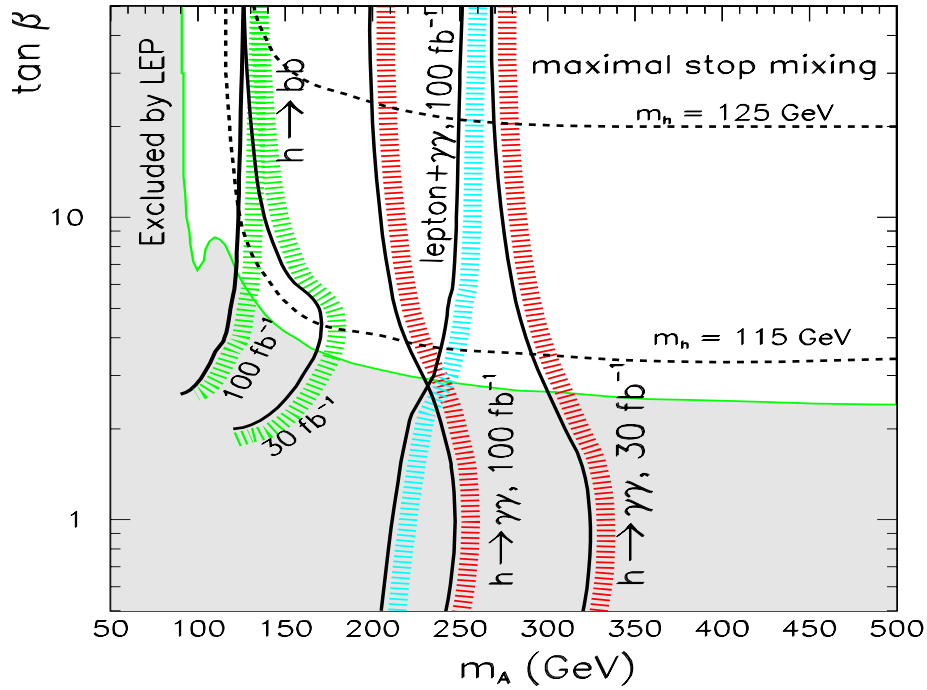
Figure 17: The same as in Fig. 16 but with maximal stop mixing. The dashed lines are the isomass curves for m_h = 115 GeV and for m_h = 125 GeV.
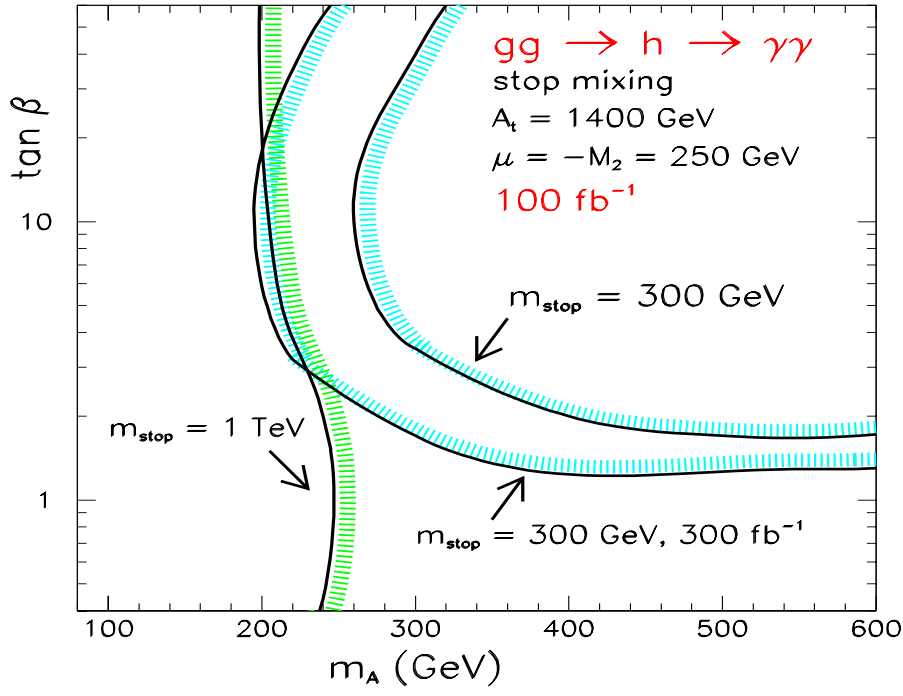
Figure 18: Expected 5σ discovery reach for $gg \to h \to \gamma\gamma$ as a function of m_A and $tan\beta$ with light stop, m_{stop} = 300 GeV, and large mixing, $A_t = 1400$ GeV for 100 and 300 fb^{-1} compared with the expectation with a heavy stop for 300 fb^{-1}.
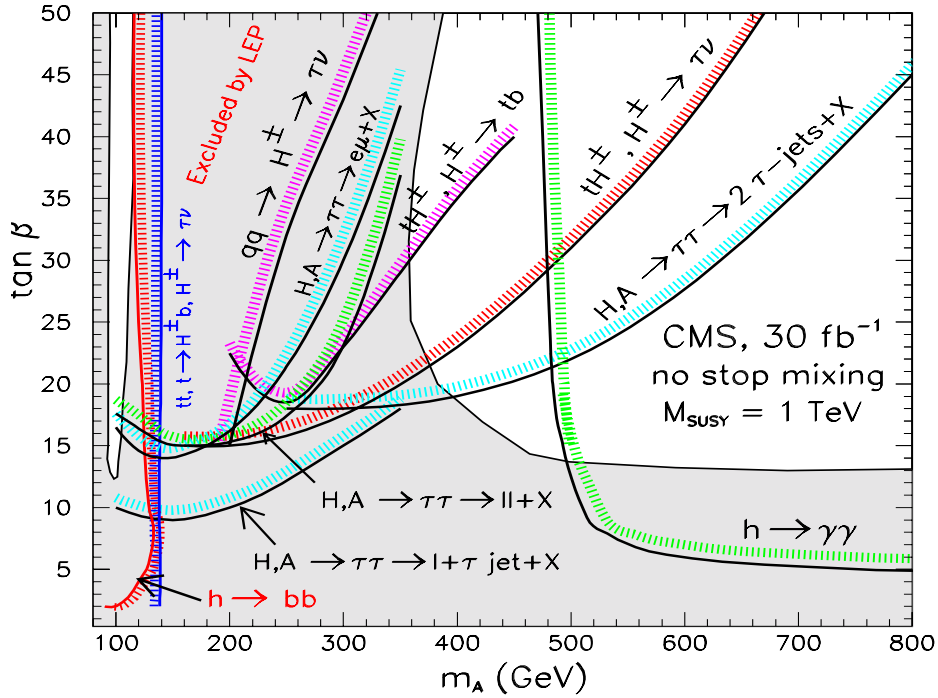
Figure 19: Expected 5σ discovery reach for the MSSM Higgs bosons in CMS in the no-mixing scenario with $30fb^{-1}$ as a function of m_A and $tan\beta$. The shaded area is excluded by LEP [1, 2]
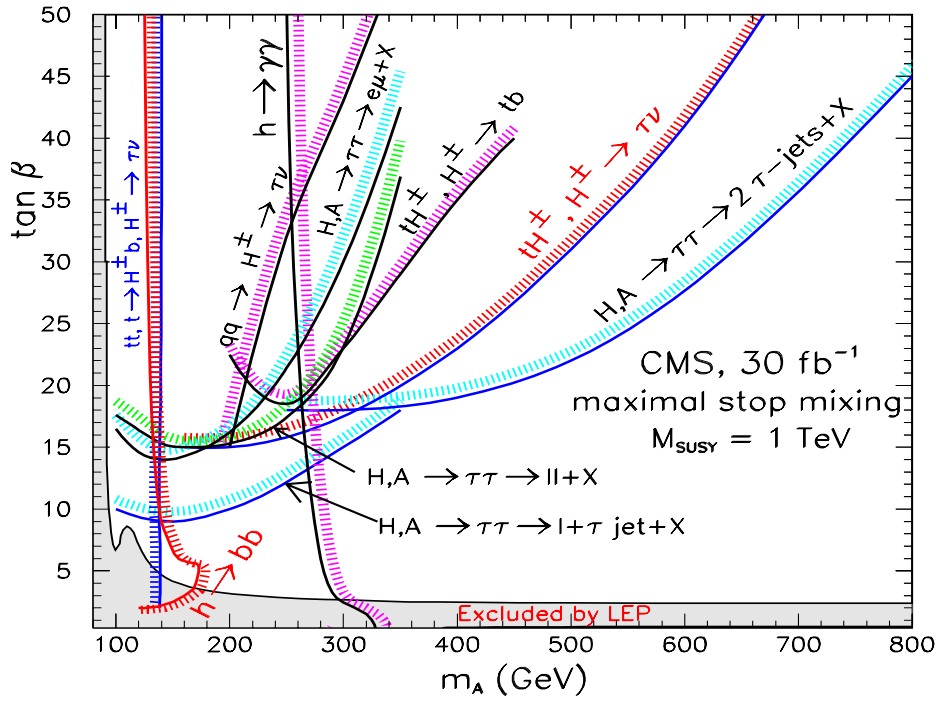
16

Figure 20: Expected 5σ discovery reach for the MSSM Higgs bosons in CMS in the maximal mixing scenario for $30 fb^{-1}$ as a function of m_A and $tan\beta$. The shaded area is excluded by LEP [1, 2].
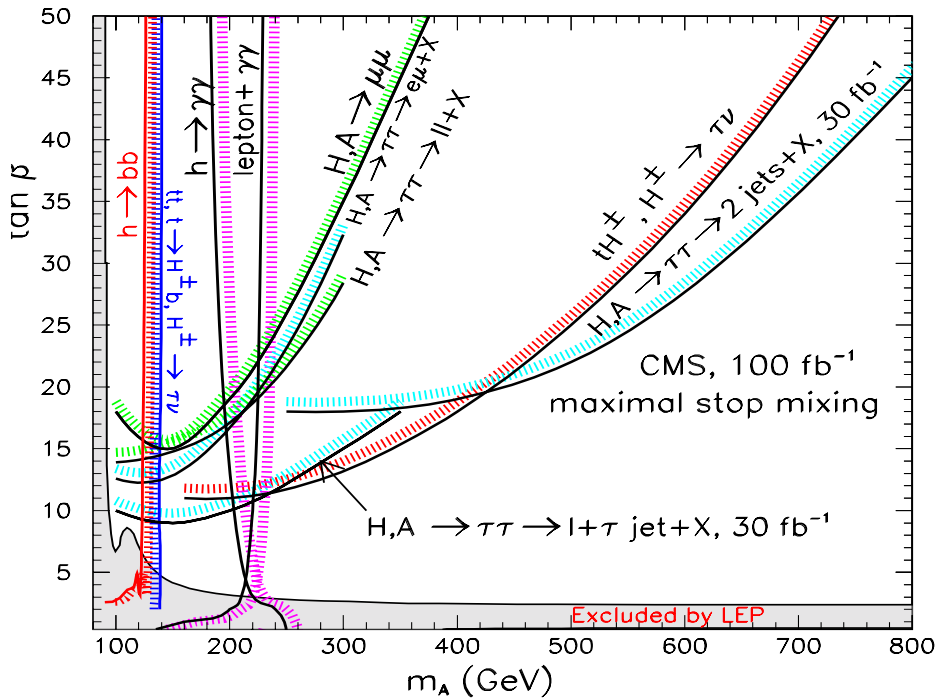
Figure 21: The same as in Fig. 20 but for $100 fb^{-1}$. The discovery reaches for $H, A \rightarrow \tau\tau \rightarrow 2\tau jets$ and for $H, A \rightarrow \tau\tau \rightarrow lepton + \tau jet$ are shown for $30 fb^{-1}$. The shaded area is excluded by LEP [1, 2]
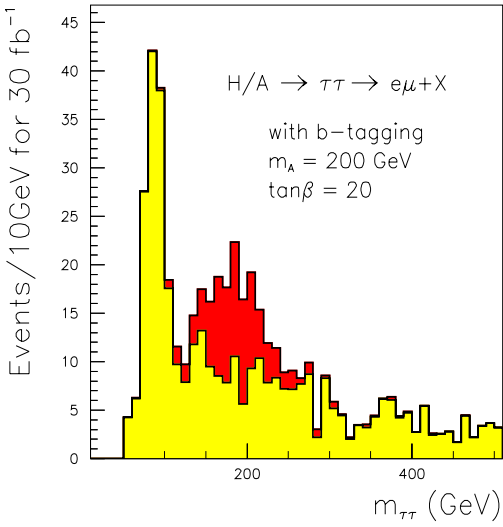
17

Figure 22: Reconstructed Higgs mass for $H, A \rightarrow \tau\tau \rightarrow e\mu$ superimposed on the total background for $m_A = 200$ GeV and $tan\beta = 20$ for 30 fb^{-1} [31].
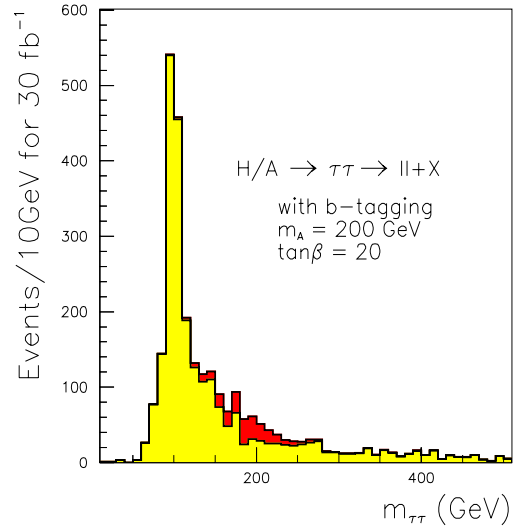
Figure 23: Reconstructed Higgs mass for $H, A \rightarrow \tau\tau \rightarrow \ell^+\ell-$ superimposed on the total background for $m_A = 200$ GeV and $tan\beta = 20$ for 30 fb^{-1} [31].
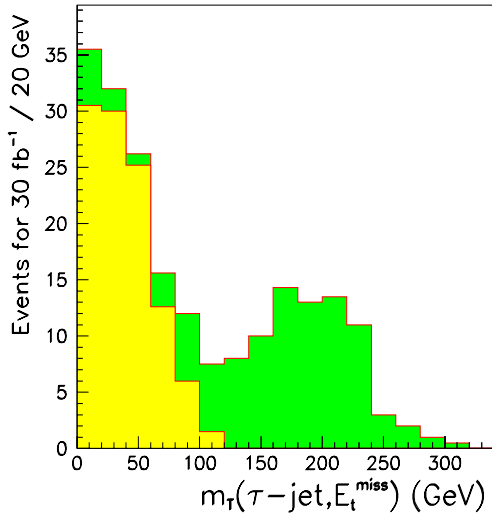

Figure 24: Reconstructed transverse mass for the charged Higgs in $tH^\pm$, $H^\pm \rightarrow \tau\nu$ with hadronic τ and top decays superimposed on the total background for $m_{H^\pm} = 217$ GeV and $tan\beta = 40$ for 30 fb^{-1}
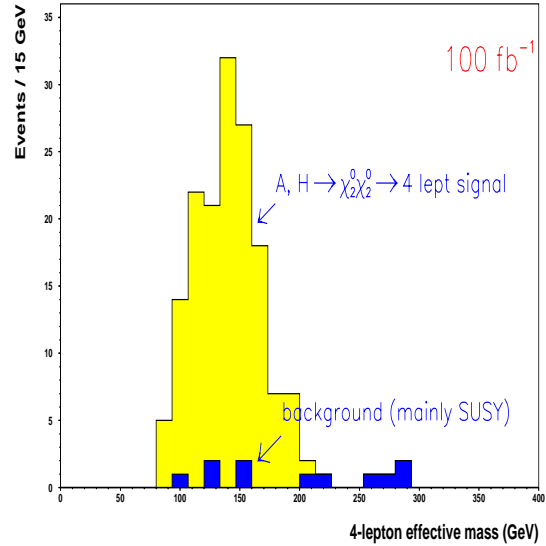
Figure 25: Invariant $4\ell^\pm$ mass for $A, H \rightarrow \chi_2^0\chi_2^0 \rightarrow 4\ell^\pm + X$ superimposed on the total SM and SUSY backgrounds for $m_A = 350$ GeV and $tan\beta = 5$ and with $M_1 = 60$ GeV, $M_2 = 120$ GeV, $\mu = -500$ GeV, $M_{\tilde{q},\tilde{g}} = 1000$ GeV, $M_{\tilde{\ell}} = 250$ GeV and $A_t = 0$
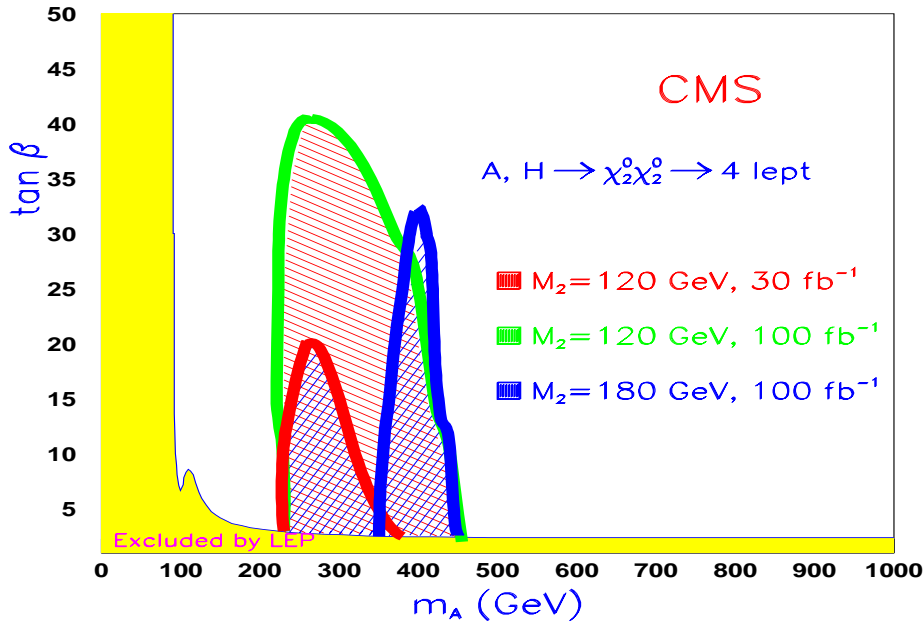
18

Figure 26: Expected 5σ discovery reach for $H, A \rightarrow \chi_2^0\chi_2^0 \rightarrow 4l^{\pm}$ as a function of m_A and $tan\beta$ with $M_1 = 60$ GeV, $M_2 = 120$ GeV, $\mu = -500$ GeV, $M_{\tilde{\ell}} = 250$ GeV, $M_{\tilde{q},\tilde{g}} = 1000$ GeV, for 30 and 100 fb^{-1}. The discovery reach assuming $M_2 = 180$ GeV is also shown for 100 fb^{-1}.
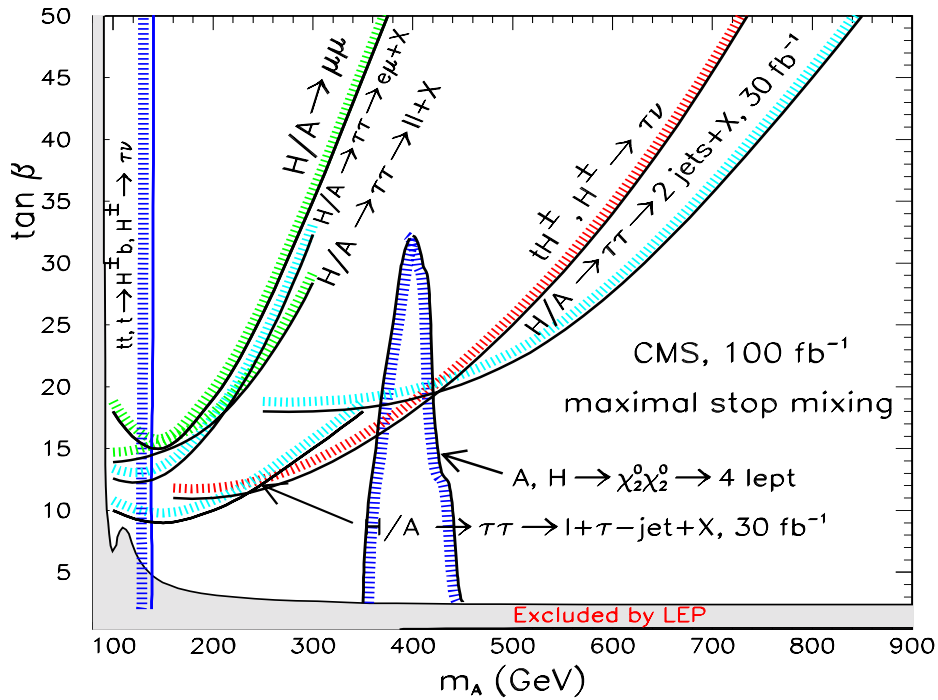

Figure 27: Expected 5σ discovery reach for the heavy MSSM Higgs bosons including $H, A \rightarrow \chi_2^0\chi_2^0 \rightarrow 4l^{\pm}$ as a function of m_A and $tan\beta$ for $100fb^{-1}$ assuming $M_1 = 90$ GeV, $M_2 = 180$ GeV, $\mu = 500$ GeV, $M_{\tilde{\ell}} = 250$ GeV, $M_{\tilde{q},\tilde{g}} = 1000$ GeV.

19